CHEMISTRY JOURNAL OF MOLDOVA. General, Industrial and Ecological Chemistry. 2023, 18(1), 70-76
ISSN (p) 1857-1727 ISSN (e) 2345-1688
http://cjm.ichem.md
http://doi.org/10.19261/cjm.2022.1021

A NEW 2D COORDINATION POLYMER BASED ON ZINC(II), 1,2,3-BENZENETRICARBOXYLIC ACID AND 4,4′-BIS(IMIDAZOL-1-YLMETHYL)BIPHENYL: SYNTHESIS AND CRYSTAL STRUCTURE

Irina Voda

Institute of Chemistry, State University of Moldova, 3, Academiei str., Chisinau MD 2028, Republic of Moldova
e-mail: irina.voda@ichem.md; iravoda@gmail.com; phone: (+373 22) 739 722

Abstract. The solvothermal reaction of zinc(II) nitrate with 1,2,3-benzenetricarboxylic acid (1,2,3-H_3BTC) and 4,4′-bis(imidazol-1-ylmethyl)biphenyl (BIBPh) produced a crystalline solid $\{[Zn_3(BIBPh)_3(BTC)_2]\cdot H_2O\}_n$. The product has been structurally characterised and investigated by X-ray diffraction, IR and thermogravimetric methods. The polymer has a bidimentional structure and crystallizes in the $P2_1/c$ space group of the monoclinic system with the following unit cell parameters: a= 14.8687(16), b= 36.915(4), c= 13.8378(16) (Å), β= 105.584(6)°. The asymmetric unit of the crystal structure contains three zinc(II) ions, three BIBPh ligands and two BTC^{3-} monodentate ligands with all three deprotonated carboxylate groups that balance the overall charge. All zinc centers have similar coordination environment: each metal ion is four coordinated exhibiting a slightly distorted tetrahedral coordination, where two positions are occupied by oxygen atoms of the carboxylic acid and the other two by nitrogen atoms of imidazole subunits.

Keywords: coordination polymer, X-ray diffraction, zinc, 1,2,3-benzenetricarboxylic acid, 4,4′-bis(imidazol-1-ylmethyl)biphenyl.

Received: 20 October 2022/ Revised final: 10 March 2023/ Accepted: 14 March 2023

Introduction

Coordination polymers are comprised of metal ions interconnected *via* multitopic ligands to create one-, two- or three-dimensional structures [1,2]. Controlled engineering of crystalline materials is still very much at the incipient stage, but certain protocols are recognised for the creation of well-defined coordination polymer structures [3-6]. A 1D network can be viewed as a chain-line structure where ditopic ligands link together metal ions that prefer, for example, a two coordinate geometry (*e.g.*, Ag(I)) [7]. A trigonal planar or square planar metal ion arrangement can facilitate the formation of a 2D network, whereas tetrahedral/octahedral metal ions are more inclined to propagate 3D networks [8-11]. Organic carboxylates, for instance, are extremely versatile building blocks which offer disparate binding modes just from the single subunit [12]. For example, there are numerous examples of metal ion-containing structures displaying μ_2-bridging [13], μ_3-bridging [14], monocationic [15] and dicationic binding modes [16]. There is also the added bonus that different di-, tri- or even tetra-carboxylic acids can be used as building blocks [17]. There is, therefore, reasonably reliable control for the formation of versatile di- and tri-dimensional networks using the carboxylate unit [18]. For the construction of metal organic frameworks (MOFs) the organic ligand that connects the metal ion coordination polyhedra is especially important since it governs the size of any generated pore [19,20]. Although 4,4'-bipyridyl was one of the most popular ligands used [21,22] other types of heterocyclic ligands have grown in popularity leading to utilisation of the 4,4′-*bis*(imidazol-1-ylmethyl)biphenyl (BIBPh) by various research groups in the design and synthesis of coordination polymers containing different transition metal ions [23,24].

The metal-organic frameworks (MOFs) are the most highly studied coordination polymers for numerous applications such as gas storage, sieving, optics, catalysis, molecular adsorption, ion exchange, sensing, magnetism, electrical conductors, monolayer films [25-35]. Also these compounds offer a unique platform for the development of solid state luminescent materials as they have an increased degree of structural predictability, in addition to well-defined environments for lumophores in crystalline form [36]. Luminescence favours prominently in coordination polymers with transition-metal ions

without unpaired electrons, especially those having d^{10} configurations and conjugated linkers with π–π stacking between adjacent rings or between the MOF and guest molecules, mostly nitrogen or oxygen-containing bridging ligands. Recently has been reported that benzenedi- or -tricarboxylates can exhibit luminescence properties in coordination polymers with zinc or cadmium metal nodes [37,38].

Lately, the research effort was focused on the use of some *3d* metals and polycarboxylate acids together with different (bis)imidazole bridging ligands in order to produce pore-like structures [39-41]. As an extension to this research topic, the aim of the present study was to obtain the coordination polymer using zinc(II) ions, BIBPh ligand and tridentate 1,2,3-benzenetricarboxylic acid (1,2,3-H_3BTC) and its structural characterisation by means of IR and thermogravimetric methods.

Experimental

Materials

All used reagents were of analytical grade and were used as received without further purification. The ligand BIBPh was prepared as reported previously [42].

Synthesis of {[Zn_3(BIBPh)$_3$($BTC)_2$]·H_2O}$_n$

A solution of BIBPh (78.5 mg, 0.25 mmol) in ethanol (2 mL) was added to the mixture of $Zn(NO_3)_2{\cdot}6H_2O$ (0.74 mg, 0.25 mmol), 1,2,3-benzenetricarboxylic acid (1,2,3-$H_3BTC{\cdot}2H_2O$) (61 mg, 0.25 mmol), NaOH (30 mg, 0.75 mmol), and distilled water (4 mL). The resulting mixture was sealed in a Teflon-lined stainless-steel vessel (10 mL) and heated at 160°C for 3 days and then cooled slowly to room temperature. Colourless crystals were filtered off and washed with water and ethanol, then dried in air. Yield: 117 mg, 89.34% (based on Zn salt). Anal. calc. for $C_{78}H_{62}N_{12}O_{13}Zn_3$ (%): C, 59.61; H, 3.98; N, 10.70. Found: C, 59.39; H, 4.13; N, 10.74. IR (ν, cm^{-1}): 3483 br, 3119 m, 2989 w, 1620 s, 1591 s, 1565 vs, 1530 s, 1502 s, 1453 s, 1443 s, 1388 vs, 1351 vs, 1285 m, 1234 m, 1188 w, 1156 w, 1102 s, 1093 s, 1071 m, 1031 m, 1005 w, 951 m, 930 w, 888 m, 843 m, 819 m, 797 s, 768 s, 747 vs, 707 s, 657 m.

Physical measurements

Elemental analysis was performed on a Vario-EL-III elemental analyzer.

IR spectrum was recorded on a Perkin Elmer Spectrum 100 spectrophotometer in the range 4000–650 cm^{-1} at room temperature. Intensities are presented as: br= broad, vs= very strong, s= strong, m= medium, w= weak.

Thermogravimetric analysis was carried out on Derivatograph Q-1500 D thermal analyzer in the range of 20–1000°C under atmospheric conditions, at a heating rate of 5°C min^{-1}.

X-ray crystallography measurements for the compound {[Zn_3(BIBPh)$_3$($BTC)_2$]·H_2O}$_n$ were carried out on a APEX-II CCD diffractometer, at 150 K, using graphite monochromated MoK_α radiation (λ= 0.71073 Å). The data were processed using SAINT software [43]. The structure was solved with the ShelXT program using intrinsic phasing method and refined by the full-matrix least-squares method on F2 with ShelXL [44,45]. Olex2 was used as an interface to the ShelX programs [46]. Non-hydrogen atoms were refined anisotropically. Aromatic hydrogen atoms were positioned geometrically and refined using a riding model. Specific details of each refinement are given in the crystallographic information files (CCDC No. 2178548).

Results and discussion

While many bridging ligands serving as pillar units connecting metal centers in polymeric networks are derived from 4,4′-bipyridyl, greater geometrical flexibility is achieved by inserting other organic groups between the two pyridyl rings and these two rings themselves may be replaced by other coordinating aromatic or aliphatic amine functions to give greater variety of chemical behaviour. The BIBPh ligand in which two imidazole rings are connected through methylene linkages to a central biphenyl ring in 4,4'-substitution provides a considerable degree of geometrical flexibility by rotation about four C–C single bonds. BIBPh has been widely used as a bridging ligand as mentioned before. Despite the flexibility of the ligand, there is a marked tendency for an anti conformation, which is defined in terms of the pseudo-torsion angle N–C…C–N formed by the two (imidazole)N–C(methylene) bonds when viewed along the C…C vector, the others have a pseudo-torsion angle within ±18° of 180° and others being rather evenly spread over other values. An anti conformation extends BIBPh to its maximum effective length as a pillar, thus providing an opportunity for the generation of significant cavities within MOFs and other coordination polymer structures.

Crystal structure

Detailed crystallographic data for {[Zn_3(BIBPh)$_3$($BTC)_2$]·H_2O}$_n$ are provided in Table 1, while the values of bond distances and angles are summarized in Table 2.

The obtained crystallographic structure is presented in Figure 1. The asymmetric unit comprises three Zn(II) metal cations, three neutral bidentate-bridging BIBPh units, two BTC^{3-} deprotonated ligands and one interstitial water molecule. The charge balance is in agreement with the formation of $\{[Zn_3(BIBPh)_3(BTC)_2]\cdot H_2O\}_n$ species, the structure of which is characterized as a two-dimensional coordination polymer (Figure 2). Two crystallographic independent BTC^{3-} ligands fulfil a tridentate-bridging function, wherein each carboxylate group behaves as a monodentate group. The interatomic separation between the Zn(II) atoms bridged by BTC^{3-} ligand: Zn1⋯Zn2, Zn2⋯Zn3, and Zn1⋯Zn3 are of 6.916(6) Å, 4.311(1) Å, and 9.474(1) Å, respectively. All the Zn ions exhibit a slightly distorted tetrahedral coordination provided by two carboxylate oxygen and two imidazole nitrogen atoms.

The crystal structure is built up from the packing of 2D coordination networks oriented parallel to the *ac* plane (Figure 3). Such a dense packing within the coordination networks is responsible for the lack of free space which could be filled by solvent molecules. As estimated by the Olex2 routine (for probe radius of 1.2 Å and resolution of 0.2 Å) the solvent accessible voids are of 632 $Å^3$, which constitutes 8.7% from the unit cell volume.

Table 1

Crystallographic parameters and the data collection statistics for the $\{[Zn_3(BIBPh)_3(BTC)_2]\cdot H_2O\}_n$.

Parameters	*Value*
Empirical formula	$C_{78}H_{62}N_{12}O_{13}Zn_3$
Formula weight, *M*	1571.50
Temperature (K)	150
Crystal system	monoclinic
Space group	$P2_1/c$
Z	4
a (Å)	14.8687(16)
b (Å)	36.915(4)
c (Å)	13.8378(16)
β (°)	105.584(6)
V ($Å^3$)	7316.0(14)
ρ_{calc} (g cm^{-3})	1.427
μ (mm^{-1})	1.048
F(000)	3232.0
Cristal size (mm^3)	0.05×0.04×0.03
2*Θ* range (°)	3.248-45.958
Limiting indices	$-16\leq h\leq 16$ $-40\leq k\leq 40$ $-15\leq l\leq 15$
Reflections collected	80455
Reflections with [$I>2\sigma(I)$]	10093
Data/restraints/ parameters	10093/6/934
Goodness-of-fit on F^2	1.056
R_1, wR_2[$I>2\sigma(I)$]	R_1= 0.0604, wR_2= 0.1247
R_1, wR_2(all data)	R_1= 0.0925, wR_2= 0.1381
Largest difference in peak and hole (e $Å^{-3}$)	1.05/-0.46

Table 2

Selected bond lengths (Å) and angles (°) for $\{[Zn_3(BIBPh)_3(BTC)_2]\cdot H_2O\}_n$.

Bond	*d* (Å)	*Bond*	*d* (Å)	*Bond*	*d* (Å)
Zn1-N1	2.022(5)	Zn2-N8^{ii}	2.028(5)	Zn3-N5	2.002(5)
Zn1-N4^{iii}	2.039(5)	Zn2-N12^{i}	2.028(5)	Zn3-N9	1.992(5)
Zn1-O1	1.971(4)	Zn2-O4	1.977(4)	Zn3-O5	1.969(4)
Zn1-O12^{iv}	1.984(4)	Zn2-O8	1.954(4)	Zn3-O9	2.031(4)
Angle	*ω* (º)	*Angle*	*ω* (º)	*Angle*	*ω* (º)
N1-Zn1-N4^{iii}	116.69(18)	N5-Zn3-O9	98.67(18)	C38-N8-Zn2^{vi}	128.3(4)
O1-Zn1-N1	101.17(17)	N9-Zn3-N5	117.0(2)	C39-N8-Zn2^{vi}	126.3(4)
O1-Zn1-N4^{iii}	98.78(18)	N9-Zn3-O9	127.05(18)	C41-N9-Zn3	125.1(4)
O1-Zn1-O12^{iv}	140.25(17)	O5-Zn3-N5	110.13(19)	C43-N9-Zn3	130.0(4)
O12^{iv}-Zn1-N1	102.69(18)	O5-Zn3-N9	104.43(19)	C58-N12-Zn2^{vii}	126.9(4)
O12^{iv}-Zn1-N41	98.28(17)	O5-Zn3-O9	97.48(17)	C60-N12-Zn2^{vii}	127.0(4)
N8^{ii}-Zn2-N12^{i}	104.90(19)	C1-N1-Zn1	124.5(4)	C61-O1-Zn1	113.0(4)
O4-Zn2-N8^{ii}	110.55(18)	C2-N1-Zn1	130.0(4)	C68-O4-Zn2	108.1(3)
O4-Zn2-N12^{i}	96.46(17)	C18-N4-Zn1^{v}	122.3(4)	C69-O5-Zn3	116.5(4)
O8-Zn2-N8^{ii}	114.55(18)	C20-N4-Zn1^{v}	131.9(4)	C70-O8-Zn2	116.7(4)
O8-Zn2-N12^{i}	109.52(18)	C22-N5-Zn3	129.1(4)	C77-O9-Zn3	103.6(4)
O8-Zn2-O4	118.45(17)	C21-N5-Zn3	124.5(4)	C78-O12-Zn1^{viii}	104.9(4)

Symmetry transformations used to generate equivalent atoms: ^{i}x-1,y,z; ^{ii}x-1,0.5-y,0.5+z; ^{iii}x-1,y,z-1; ^{iv}x,y,z+1; ^{v}x+1,y,z+1; ^{vi}x+1,0.5-y, z-0.5; ^{vii}x+1,y,z; ^{viii}x,y,z-1.

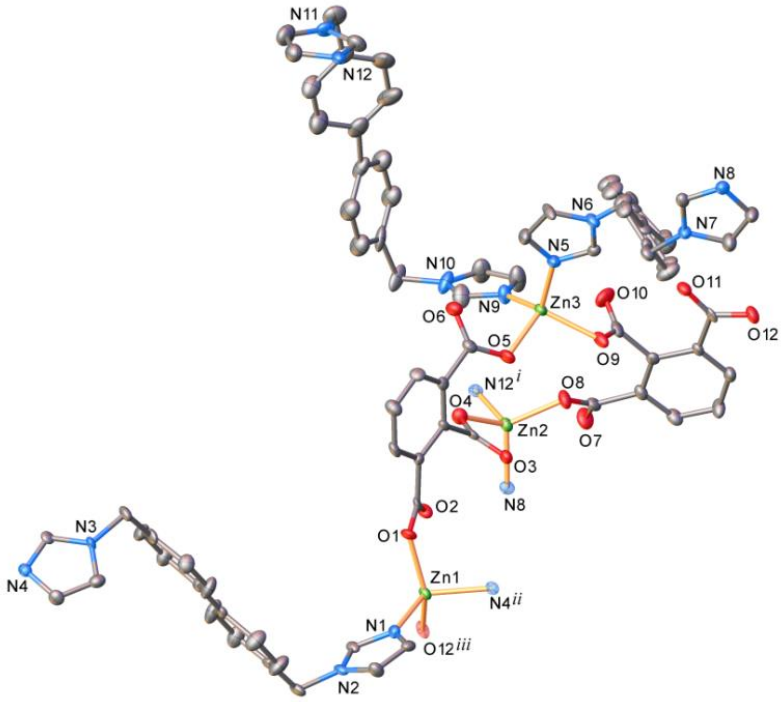

Figure 1. Extended view of the asymmetric part in the crystal structure of $\{[Zn_3(BIBPh)_3(BTC)_2]\cdot H_2O\}_n$ along with atom labelling and thermal ellipsoids at the 50% level. Hydrogen atoms were omitted for clarity. Symmetry generated fragments are shown with faded colours. Symmetry codes: $^{i)}x - 1, y, z$; $^{ii)}x - 1, 0.5 - y, 0.5 + z$; $^{iii)}x - 1, y, z - 1$. (For interpretation of the references to color in this figure legend, the reader is referred to the Web version of this article.)

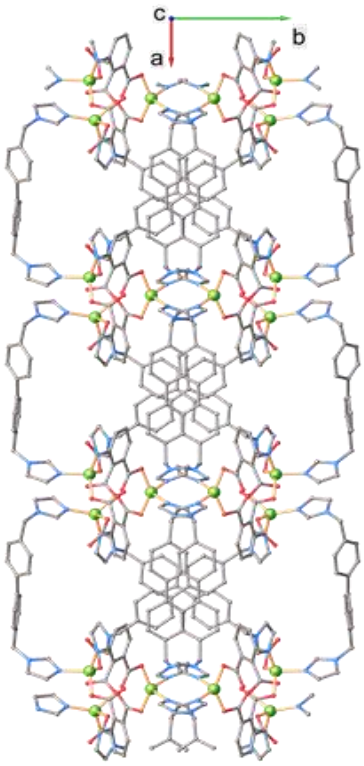

Figure 2. The 2D coordination polymer $\{[Zn_3(BIBPh)_3(BTC)_2]\cdot H_2O\}_n$ viewed along *c* axis. H-atoms are not shown.

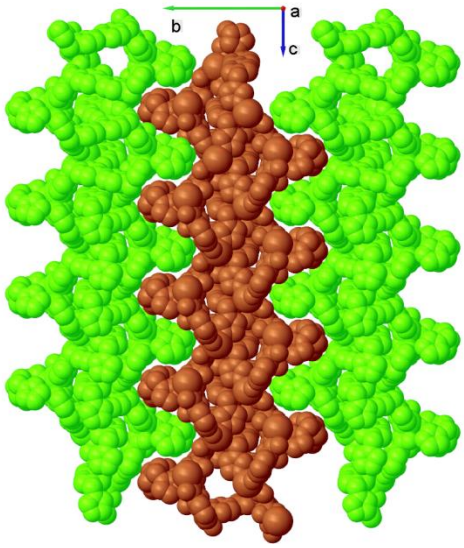

Figure 3. Partial view of the crystal structure along *a* axis, showing the parallel packing of 2D networks.

IR spectroscopic characterization

The presence of co-crystallized water molecules in the obtained compound structure is shown by broad IR band in the 3700–3200 cm^{-1} range. IR spectroscopy for this compound also clearly indicates the presence of monodentate carboxylate groups with both asymmetric and symmetric stretching modes: bands at 1620 and 1388 cm^{-1} correspond to stretching vibrations $\nu_{as}(COO^-)$ and $\nu_s(COO^-)$ respectively for a carboxylate group. The difference between asymmetric and symmetric carboxylate stretching frequencies (Δ= [$\nu_{as}(COO^-)$–$\nu_s(COO^-)$]= 1620–1388= 232 cm^{-1}) is consistent with carboxylate groups coordinating through only one O atom [47]. The C–H stretches give rise to the bands in the 3119–2989 cm^{-1} region, and the features of the 1285–657 cm^{-1} range represent the fingerprint region of the substituted ligand rings.

Thermogravimetric analysis

The coordination polymer network robustness and the removal of water molecules are shown by the TGA trace, Figure 4. According to the TGA plot, an initial small mass loss of 1% until 130°C corresponds to the facile removal of uncoordinated water molecules (calculated: 1.5%). The plateau thereafter demonstrates that the dehydrated coordination network is stable up to 280°C, above which extensive decomposition occurs in 4 stages; the final residue is ZnO (calculated: 15.45%).

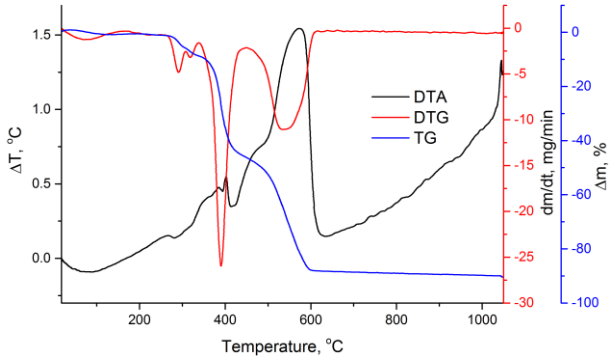

Figure 4. The TG/DTG/DTA curves of the compound recorded in the range of 20–1000°C under atmospheric conditions.

Conclusions

The ligand BIBPh offers the ability to bridge metal ion centers in a pillar-like way, facilitating the formation of coordination polymers and metal-organic frameworks of various dimensionalities depending on coordination geometry and the presence of other ligands. Although it is found most often in crystal structures in anti conformation, it has sufficient flexibility to adapt to preferences and restrictions imposed by the other structural components and thus to adopt other conformations.

The three carboxylate groups of BTC^{3-} providing structural flexibility and different conformations of the BIBPh ligand joining zinc ions gives rise to a new 2D coordination polymer with cavities generated in the structure occupied by water molecules. These structural features, revealed by X-ray crystallography, are confirmed by IR spectroscopy and thermogravimetric analysis.

Acknowledgements

This work was realized under the supervision of late Professor Constantin Turta (20.12.1940-23.03.2015).

The author is deeply thankful to Professor Christoph Janiak group of Düsseldorf University for the X-ray analysis measurement.

Also, the author expresses gratitude to Dr. Sergiu Shova for advices regarding crystallographic structure determination.

Funding

This work was funded by the Project ANCD/20.80009.5007.04. “New materials based on coordination compounds of metals with polyfunctional ligands as porous polymers, catalysts, biologically active substances and nanostructured compounds”.

References

1. Moulton, B.; Zaworotko, M.J. From molecules to crystal engineering: supramolecular isomerism and polymorphism in network solids. Chemical Reviews, 2001, 101(6), pp. 1629–1658. DOI: https://doi.org/10.1021/cr9900432
2. James, S.L. Metal-organic frameworks. Chemical Society Reviews, 2003, 32(5), pp. 276–288. DOI: https://doi.org/10.1039/B200393G
3. Hagrman, P.J.; Hagrman, D.; Zubieta, J. Organic-inorganic hybrid materials: from „simple” coordination polymers to organodiamine-templated molybdenum oxides. Angewandte Chemie International Edition, 1999, 38(17), pp. 2639–2684. DOI: https://doi.org/10.1002/(SICI)1521-3773(19990917)38:18<2638::AID-ANIE2638>3.0.CO;2-4
4. Robson, R. A net-based approach to coordination polymers. Journal of the Chemical Society, Dalton Transactions, 2000, 21, pp. 3735–3744. DOI: https://doi.org/10.1039/B003591M
5. Yaghi, O.M.; O'Keeffe, M.; Ockwig, N.W.; Chae, H.K.; Eddaoudi, M.; Kim, J. Reticular synthesis and the design of new materials. Nature, 2003, 423, pp. 705–714. DOI: https://doi.org/10.1038/nature01650
6. Kitagawa, S.; Kitaura, R.; Noro, S. Functional porous coordination polymers. Angewandte

Chemie International Edition, 2004, 43(18), pp. 2334–2375.
DOI: https://doi.org/10.1002/anie.200300610
7. Wang, D.; He, H.; Chen, X.; Feng, S.; Niu, Y.; Sun, D. A 3D porous metal–organic framework constructed of 1D zigzag and helical chains exhibiting selective anion exchange. CrystEngComm, 2010, 12(4), pp. 1041–1043.
DOI: https://doi.org/10.1039/B910988A
8. Jana, S.; Chattopadhyay, S. Design and construction of copper(I) complexes based on flexi-dentate cyclic N_2-donor Schiff bases *via in situ* reduction of copper(II) precursors. Polyhedron, 2014, 81, pp. 298–307.
DOI: https://doi.org/10.1016/j.poly.2014.05.083
9. Lu, J.Y.; Babb, A.M. The first triple-layer 2-D coordination polymer: $[Cu_3(bpen)(IN)_6(H_2O)_2]$. Inorganic Chemistry, 2001, 40(14), pp. 3261–3262.
DOI: https://doi.org/10.1021/ic015531i
10. Furukawa, H.; Ko, N.; Go, Y.B.; Aratani, N.; Choi, S.B.; Choi, E.; Yazaydin, A.Ö.; Snurr, R.Q.; O'Keeffe, M.; Kim, J.; Yaghi, O.M. Ultrahigh porosity in metal-organic frameworks. Science, 2010, 329(5990), pp. 424–428.
DOI: https://doi.org/10.1126/science.1192160
11. Yi, F.-Y.; Dang, S.; Yang, W.; Sun, Z.-M. Construction of porous Mn(II)-based metal–organic frameworks by flexible hexacarboxylic acid and rigid coligands**.** CrystEngComm, 2013, 15(41), pp. 8320–8329.
DOI: https://doi.org/10.1039/C3CE41406J
12. Tranchemontagne, D.J.; Mendoza-Cortés, J.L.; O'Keeffe, M.; Yaghi, O.M. Secondary building units, nets and bonding in the chemistry of metal-organic frameworks. Chemical Society Reviews, 2009, 38(5), pp. 1257–1283.
DOI: https://doi.org/10.1039/B817735J
13. Rixson, D.; Sezer, G.G.; Alp, E.; Mahon, M.F.; Burrows, A.D. Synthesis, structures and properties of metal–organic frameworks prepared using a semi-rigid tricarboxylate linker. CrystEngComm, 2022, 24, pp. 863–876.
DOI: https://doi.org/10.1039/D1CE01284C
14. Gavilan, E.; Audebrand, N.; Jeanneau, E. A new series of mixed oxalates $MM'(C_2O_4)_3(H_2O)_3{\cdot}nH_2O$ (M= Cd, Hg, Pg; M′ = Zr, Hf) based on eight-fold coordinated metals: synthesis, crystal structure from single-crystal and powder diffraction data and thermal behaviour. Solid State Sciences, 2007, 9(11), pp. 985–999. DOI: https://doi.org/10.1016/j.solidstatesciences.2007.07.024
15. Gelbrich, T.; Threlfall, T.L.; Huth, S.; Seeger, E. Structures of racemic lithium tartrate hydrates. Polyhedron, 2006, 25(4), pp. 937–944.
DOI: https://doi.org/10.1016/j.poly.2005.10.021
16. Murugavel, R.; Karambelkar, V.V.; Anantharaman, G.; Walawalkar, M.G. Synthesis, spectral characterization, and structural studies of 2-aminobenzoate complexes of divalent alkaline earth metal ions: X-ray crystal structures of $[Ca(2\text{-aba})_2(OH_2)_3]_\infty$, $[\{Sr(2\text{-aba})_2(OH_2)_2\}{\cdot}H_2O]_\infty$, and $[Ba(2\text{-aba})_2(OH_2)]_\infty$ (2-abaH = 2-$NH_2C_6H_4COOH$). Inorganic Chemistry, 2000, 39(7), pp. 1381–1390.
DOI: https://doi.org/10.1021/ic990895k
17. Perry, J.J.; Perman, J.A.; Zaworotko, M.J. Design and synthesis of metal-organic frameworks using metal-organic polyhedra as supermolecular building blocks. Chemical Society Reviews, 2009, 38(5), pp. 1400–1417.
DOI: https://doi.org/10.1039/B807086P
18. Prior, T.J.; Rosseinsky, M.J. Crystal engineering of a 3-D coordination polymer from 2-D building blocks. Chemical Communications, 2001, 5, pp. 495–496.
DOI: https://doi.org/10.1039/B009455M
19. Eddaoudi, M.; Kim, J.; Rosi, N.; Vodak, D.; Wachter, J.; O'Keeffe, M.; Yaghi, O.M. Systematic design of pore size and functionallity in isoreticular MOFs and their application in methane storage. Science, 2002, 295(5554), pp. 469–472.
DOI: http://dx.doi.org/10.1126/science.1067208
20. Deng, H.; Grunder, S.; Cordova, K.E.; Valente, C.; Furukawa, H.; Hmadeh, M.; Gándara, F.; Whalley, A.C.; Liu, Z.; Asahina, S.; Kazumori, H.; O'Keeffe, M.; Terasaki, O.; Stoddart, J.F.; Yaghi, O.M. Large-pore apertures in a series of metal-organic frameworks. Science, 2012, 336(6084), pp. 1018–1023.
DOI: http://dx.doi.org/10.1126/science.1220131
21. Gable, R.W.; Hoskins, B.F.; Robson, R. A new type of interpenetration involving enmeshed independent square grid sheets. The structure of diaquabis-(4,4′-bipyridine)zinc hexafluorosilcate. Journal of the Chemical Society, Chemical Communications, 1990, 23, pp. 1677–1678.
DOI: https://doi.org/10.1039/C39900001677
22. Liu, B.; Xu, L. A novel 3-D metal-organic framework constructed from a negative 2-D layer $[Cu_2(BTB)_2]^{2-}$ and long linkers $[Cu(4,4'\text{-bipy})_2]^{2+}$: synthesis, crystal structure and blue fluorescence. Inorganic Chemistry Communications, 2006, 9(4), pp. 364–366.
DOI: https://doi.org/10.1016/j.inoche.2006.01.004
23. Fei, B.-L.; Sun, W.-Y.; Zhang, K.-B.; Yu, K.-B.; Tang, W.-X. Synthesis and crystal structure of an infinite one-dimensional chain containing a poly-metallocage of Mn^{II} with 4,4′-bis(imidazol-1-ylmethyl)biphenyl. Journal of the Chemical Society, Dalton Transactions, 2000, 14, pp. 2345–2348.
DOI: https://doi.org/10.1039/B002692L
24. Zhu, H.-F., Zhao, W.; Okamura, T.-A.; Fei, B.-L.; Sun, W.-Y.; Ueyama, N. Self-assembly of a snake-like blue photoluminescent coordination polymer from 4,4′-bis(imidazol-1-ylmethyl)biphenyl and zinc acetate. New Journal of Chemistry, 2002, 26(10), pp. 1277–1279.
DOI: https://doi.org/10.1039/B200383J
25. Hu, Y.H.; Zhang, L. Hydrogen storage in metal–organic frameworks. Advanced Materials, 2010, 22(20), pp. E117–E130.
DOI: https://doi.org/10.1002/adma.200902096

26. Li, J.-R.; Sculley, J.; Zhou, H.-C. Metal–organic frameworks for separations. Chemical Reviews, 2012, 112(2), pp. 869–932. DOI: https://doi.org/10.1021/cr200190s
27. Venna, S.R.; Jasinski, J.B.; Carreon, M.A. Structural evolution of zeolitic imidazolate framework-8. Journal of the American Chemical Society, 2010, 132(51), pp. 18030–18033. DOI: https://doi.org/10.1021/ja109268m
28. Zhang, X.-P.; Wang, D.-G.; Su, Y.; Tian, H.-R.; Lin, J.-J.; Feng, Y.-L.; Cheng, J.-W. Luminescent 2D bismuth–cadmium–organic frameworks with tunable and white light emission by doping different lanthanide ions. Dalton Transaction, 2013, 42(29), pp. 10384–10387. DOI: https://doi.org/10.1039/C3DT50826A
29. Farrusseng, D.; Aguado, S.; Pinel, C. Metal–organic frameworks: opportunities for catalysis. Angewandte Chemie International Edition, 2009, 48(41), pp. 7502–7513. DOI: https://doi.org/10.1002/anie.200806063
30. Zhang, X.-M.; Tong, M.-L.; Gong, M.-L.; Chen, X.-M. Supramolecular organisation of polymeric coordination chains into a three-dimensional network with nanosized channels that clathrate large organic molecules. European Journal of Inorganic Chemistry, 2003, 1, pp. 138–142. DOI: https://doi.org/10.1002/ejic.200390014
31. Chandler, B.D.; Cramb, D.T.; Shimizu, G.K.H. Microporous metal–organic frameworks formed in a stepwise manner from luminescent building blocks. Journal of the American Chemical Society, 2006, 128(32), pp. 10403–10412. DOI: https://doi.org/10.1021/ja060666e
32. Espallargas, G.M.; Coronado, E. Magnetic functionalities in MOFs: from the framework to the pore. Chemical Society Reviews, 2018, 47(2), pp. 533–557. DOI: https://doi.org/10.1039/C7CS00653E
33. Xie, L.S.; Skorupskii, G.; Dincă M. Electrically conductive metal-organic frameworks. Chemical Reviews, 2020, 120(16), pp. 8536–8580. DOI: https://doi.org/10.1021/acs.chemrev.9b00766
34. Zacher, D.; Shekhah, O.; Woll, C.; Fischer, R.A. Thin films of metal-organic frameworks. Chemical Society Reviews, 2009, 38(5), pp. 1418–1429. DOI: https://doi.org/10.1039/B805038B
35. Wang, Z.; Liu, J.; Arslan, H.K.; Grosjean, S.; Hagendorn, T.; Gliemann, H.; Brase, S.; Wöll, C. Post-synthetic modification of metal-organic framework thin films using click chemistry: the importance of strained c−c triple bonds. Langmuir, 2013, 29(51), pp. 15958–15964. DOI: https://doi.org/10.1021/la403854w
36. Allendorf, M.D.; Bauer, C.A.; Bhakta, R.K.; Houk, R.J.T. Luminescent metal–organic frameworks. Chemical Society Reviews, 2009, 38(5), pp. 1330–1352. DOI: https://doi.org/10.1039/B802352M
37. Chen, C.-J.; Ye, X.-P.; Gao, J.-Y.; Xie, W.-P.; Ran, X.-R.; Yue, S.-T.; Cai, Y.-P. Auxiliary ligand-directed synthesis of four novel functional supramolecular metal–organic frameworks from 1-D chains to 3-D architectures. Inorganic Chemistry Communications, 2013, 29, pp. 4–10. DOI: https://doi.org/10.1016/j.inoche.2012.11.031
38. Yu, Y.-H.; Wen, B.; Zhang, H.-Z.; Hou, G.-F.; Gao, J.-S.; Yan, P.-F. Construction of two interpenetrating coordination networks based on 4,4′-*bis*(1H-imidazol-1-yl-methyl)biphenyl and effect of carboxylic acids. Journal of Coordination Chemistry, 2014, 67(4), pp. 588–596. DOI: https://doi.org/10.1080/00958972.2014.895824
39. Voda, I.; Turta, C.; Lozan, V.; Benniston, A.C.; Baisch, U. Synthesis of a zinc(II) cage-like structure based on 1,4-*bis*((1H-imidazoyl-1-yl)methyl)benzene and 5-sulfoisophthalic acid. Polyhedron, 2014, 67, pp. 301–305. DOI: http://dx.doi.org/10.1016/j.poly.2013.09.002
40. Voda, I.; Makhloufi, G.; Lozan, V.; Shova, S.; Heering, C.; Janiak, C. Mixed-ligand cobalt, nickel and zinc coordination polymers based on flexible 1,4-*bis*((1H-imidazol-1-yl)methyl)benzene and rigid carboxylate linkers. Inorganica Chimica Acta, 2017, 455, pp. 118–131. DOI: http://dx.doi.org/10.1016/j.ica.2016.10.007
41. Voda, I.; Makhloufi, G.; Druta, V.; Lozan, V.; Shova, S.; Bourosh, P.; Kravtsov, V.; Janiak, C. Mixed-ligand coordination compounds based on the rigid 4,4′-*bis*(1-imidazolyl)biphenyl and pyridinedicarboxylate ligands. Inorganica Chimica Acta, 2018, 482, pp. 526–534. DOI: https://doi.org/10.1016/j.ica.2018.06.038
42. Vlahakis, J.Z.; Mitu, S.; Roman, G.; Rodriguez, E.P.; Crandall, I.E.; Szarek, W.A. The anti-malarial activity of bivalent imidazolium salts. Bioorganic & Medicinal Chemistry, 2011, 19(21), pp. 6525–6542. DOI: https://doi.org/10.1016/j.bmc.2011.06.002
43. Bruker, SAINT-Plus, version 7.06a and APEX2, Bruker-Nonius AXS Inc., Madison, WI, 2004.
44. Sheldrick, G.M. SHELXT - Integrated space-group and crystal-structure determination. Acta Crystallographica, Section A 71, 2015, pp. 3–8. DOI: https://doi.org/10.1107/S2053273314026370
45. Sheldrick, G.M. Crystal structure refinement with SHELXL. Acta Crystallographica, Section C 71, 2015, pp. 3–8. DOI: https://doi.org/10.1107/S2053229614024218
46. Dolomanov, O.V.; Bourhis, L.J.; Gildea, R.J.; Howard, J.A.K.; Puschmann, H. OLEX2: a complete structure solution, refinement and analysis program. Journal of Applied Crystallography, 2009, 42, pp. 339–341. DOI: https://doi.org/10.1107/S0021889808042726
47. Nakamoto, K. Infrared and Raman spectra of inorganic and coordination compounds. Jonh Wiley & Sons: New York, 1986, 484 p. https://www.wiley.com/en-md